Discreteness-induced slow relaxation in reversible catalytic reaction networks

Akinori Awazu[1] and Kunihiko Kaneko[2,3]
[1]*Department of Mathematical and Life Sciences, Hiroshima University, Kagami-yama 1-3-1, Higashi-Hiroshima 739-8526, Japan*
[2]*Department of Basic Science, University of Tokyo, Komaba, Meguro-ku, Tokyo 153-8902, Japan*
[3]*ERATO Complex Systems Biology, JST, Komaba, Meguro-ku, Tokyo 153-8902, Japan*
(Received 1 March 2010; revised manuscript received 15 April 2010; published 21 May 2010)

Slowing down of the relaxation of the fluctuations around equilibrium is investigated both by stochastic simulations and by analysis of master equation of reversible reaction networks consisting of reactions between a pair of resource and the corresponding high-energy product that works as a catalyst for another resource-product reaction. As the number of molecules N is decreased, the relaxation time to equilibrium is prolonged due to the deficiency of catalysts, as demonstrated by the amplification compared to that by the continuum limit. This amplification ratio of the relaxation time is represented by a scaling function as $h=N\exp(-\beta V)$, and it becomes prominent as N becomes less than a critical value $h\sim 1$, where β is the inverse temperature and V is the energy required to the transformation from resources to the corresponding products.

DOI: 10.1103/PhysRevE.81.051920 PACS number(s): 87.16.Yc, 05.40.−a, 82.39.Rt

I. INTRODUCTION

The study of reaction processes in catalytic reaction networks is generally important to understand the dynamics and fluctuations in biochemical systems and their functionality. Obviously, understanding the generic features of equilibrium characteristics and relaxation to equilibrium is the first step toward gaining such an understanding. Indeed, such reaction systems often exhibit anomalous slow relaxation to equilibrium due to some kinetic constraints such as diffusion-influenced (limited) reaction [1] and formations of transient Turing patterns [2]. In this paper, we consider a mechanism to realize such a slow relaxation in catalytic reaction networks, where the discreteness in molecule number that may reach zero induces drastic slowing down.

Most intracellular reactions progress with the aid of catalysts (proteins), whereas catalysts have to be synthesized as a result of such catalytic reactions. Indeed, reaction dynamics in catalytic networks have been extensively investigated. In most such studies, a limiting case with a strong nonequilibrium condition was assumed by adopting a unidirectional reaction process (i.e., by neglecting backward reactions). To understand the basic properties of biochemical reactions, however, it is important to study both equilibrium and nonequilibrium characteristics by including forward and backward reactions that satisfy the detailed balance condition. Such a study is not only important for statistical thermodynamics, but it also provides some insight on the regulation of synthesis or degradation reactions for homeostasis in cells.

Recently, we discovered a slow relaxation process to equilibrium, which generally appears in such catalytic reaction networks, and we proposed "chemical-net glass" as a novel class of nonequilibrium phenomena. In this case, relaxation in the vicinity of equilibrium is exponential, whereas far from it much slower logarithmic relaxation with some bottlenecks appears due to kinetic constraints in catalytic relationships [3]. In this study, we adopted continuous rate equations and assumed that the molecule number is sufficiently large.

In biochemical reaction processes, however, some chemical species can play an important role at extremely low concentrations of even only a few molecules per cell [4–6]. In such systems, fluctuations and discreteness in the molecule number are important. Indeed, recent studies by using a stochastic simulation of catalytic reaction networks have demonstrated that the smallness in the molecule number induces a drastic change with regard to statistical and spatiotemporal behaviors of molecule abundances from those obtained by the rate equation, i.e., at the limit of large molecule numbers [7–20]. In these studies, the strong nonequilibrium condition is assumed by taking a unidirectional reaction.

Now, it is important to study the relaxation process to equilibrium by considering the smallness in the molecule number. Does the discreteness in molecule number influence the equilibrium and relaxation behaviors? Is the relaxation process slowed down by the smallness in the molecule number? To address these questions, we have carried out several simulations of the relaxation dynamics of random catalytic reaction networks by using stochastic simulations. Numerical results from several networks [21,22] suggest that the relaxation time is prolonged drastically when the number of molecules is smaller. Usually, the temperature dependence of the relaxation time follows the Kramers form $\exp(\beta E)$, where β is the inverse temperature and E is a certain energy, depending on the system. When the discreteness in molecule number is relevant to the relaxation, this energy deviates from the value at the continuum limit, as the molecule number is decreased. The deviation of the relaxation time from the continuum limit is expressed by the factor $\exp(\beta\delta E)$. If δE is positive, it is considered as the effective additional energy required to pass through the bottleneck due to the discreteness in molecule number.

In this paper, we analyze such slowing down of a reaction process to equilibrium that is induced by the smallness in molecule numbers. Instead of taking complex reaction networks, we choose simple networks or network motives to estimate the relaxation time analytically. In fact, complex networks are often constructed by combining a variety of simple network motives with simple branch or loop structures. We focus on the relaxation dynamics of reversible catalytic reaction systems with such simple network motives as a first step toward understanding the general relaxation

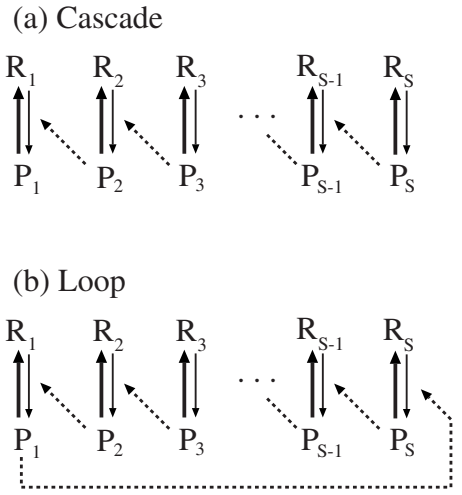

FIG. 1. Illustration of (a) cascade and (b) loop systems. Solid arrows indicate reaction paths (their width indicates the transition tendency) and dashed arrows indicate catalyzation.

properties in complex catalytic reaction networks.

In Sec. II, we introduce two network motives, where the synthesis of a product from resource molecules (and its reverse reaction) is catalyzed by one of the other products. Here, we note that some specific network motives may exhibit incomplete equilibration when the molecule number decreases, and the average chemical concentration in the steady state deviates from the equilibrium concentration derived by the continuous rate equations.

In Sec. III, we show relaxation characteristics from the stochastic simulations. The relaxation of the fluctuation around the steady state slows down as the molecule number is decreased below a critical value. The increase in the relaxation time is represented by a scaling function by using

$$h = N \exp(-\beta V),$$

where N is the molecule number and V is the energy gap between a product and a resource. In Sec. IV, we present an analytical estimate for this relaxation suppression due to the smallness in molecule number by using a suitable approximation for master equation. In Sec. V, we present a summary and discuss the generality of our results.

II. MODELS

Here, we consider reversible catalytic reaction systems with two simple network structures, cascade and loop systems, as shown in Fig. 1, which may function as network motives for complex reaction networks. These systems consist of $2S$ chemical species, S product chemicals, and S resource chemicals; and each product is transformed to the corresponding resource, and vice versa, by the catalyzation of one of the other products. Here, we assume that each product chemical can catalyze at most one of the other resource-product reactions. (Instead, we can interpret that there exist S chemical species with excited and nonexcited states, and chemicals in an excited state can catalyze an excitation reaction of one of the other molecules.) Here, we label a pair of resource and the corresponding product R_i and P_i by the following manner:

First, we choose and label a resource and the corresponding product as R_1 and P_1. Then there is one product that catalyzes this R_1-P_1 reaction. We label this product as P_2 and the resource corresponding to this product as R_2. Next, the product which catalyzes the P_2-R_2 reaction and the corresponding resource is labeled as R_3 and P_3, and so forth. Here, we define the rate of the reaction from P_i to R_i and that from R_i to P_i proceeded by the catalyst P_{i+1} as k_{P_i,R_i} and k_{R_i,P_i}. If all chemicals are catalyzed by one of them, we can write the reaction as

$$P_i + P_{i+1} \underset{k_{R_i,P_i}}{\overset{k_{P_i,R_i}}{\rightleftarrows}} R_i + P_{i+1}$$

for $i=1,2,\ldots,S-1$, where

$$P_S + P_1 \underset{k_{R_S,P_S}}{\overset{k_{P_S,R_S}}{\rightleftarrows}} R_S + P_1,$$

which leads to the loop system [Fig. 1(b)]. When there exists a product which does not catalyze any reactions and we label such a product and the corresponding resource as P_1 and R_1, the cascade system in Fig. 1(a) is obtained, where

$$P_S \underset{k_{R_S,P_S}}{\overset{k_{P_S,R_S}}{\rightleftarrows}} R_S.$$

(By neglecting cases in which some pair of resource and product is totally disconnected from others, the loop and cascade systems are the only possibilities.)

The reaction rates k_{P_i,R_i} and k_{R_i,P_i} are set so that they satisfy the detailed balance condition. We assume that the energy of the chemical P_i is larger than that of R_i, and set $k_{P_i,R_i}=1$ and $k_{R_i,P_i}=\exp(-\beta V_i)$, where V_i is the energy gap between P_i and R_i and β is the inverse temperature. We define p_i and r_i as the numbers of molecules of the chemical species P_i and R_i, respectively. We fix the total number of molecules as SN, and $p_i+r_i=N$ holds for each i. The state of the system is represented by a set of numbers $(p_1,p_2,\ldots,p_S)$.

In both the systems, it is noted that for $N\to\infty$ (i.e., the continuous limit), $\langle p_i\rangle/N \to p_i^{eq}/N = e^{-\beta V_i}/(1+e^{-\beta V_i})$ and $\langle r_i\rangle/N \to r_i^{eq}/N = 1/(1+e^{-\beta V_i})$ hold at the equilibrium distribution, which is reached at $t\to\infty$. The derivations of these equilibrium concentrations from the rate equation will be given in Sec. IV.

For finite N, however, there is a difference between the distributions of the cascade and the loop systems. In the cascade system, the average of the equilibrium chemical concentrations is identical to the continuum limit and is given by $\langle p_i\rangle/N = e^{-\beta V}/(1+e^{-\beta V})$, that is, they are independent of N and β. This is because all the states $(p_1,p_2,\ldots,p_S)$ $(0\le p_i \le N)$ are connected by reactions and the above equilibrium distribution is the only stationary solution for the master equation.

On the other hand, in the loop system, there is a deviation in the steady chemical concentration from the continuum limit, which becomes more prominent as N becomes smaller.

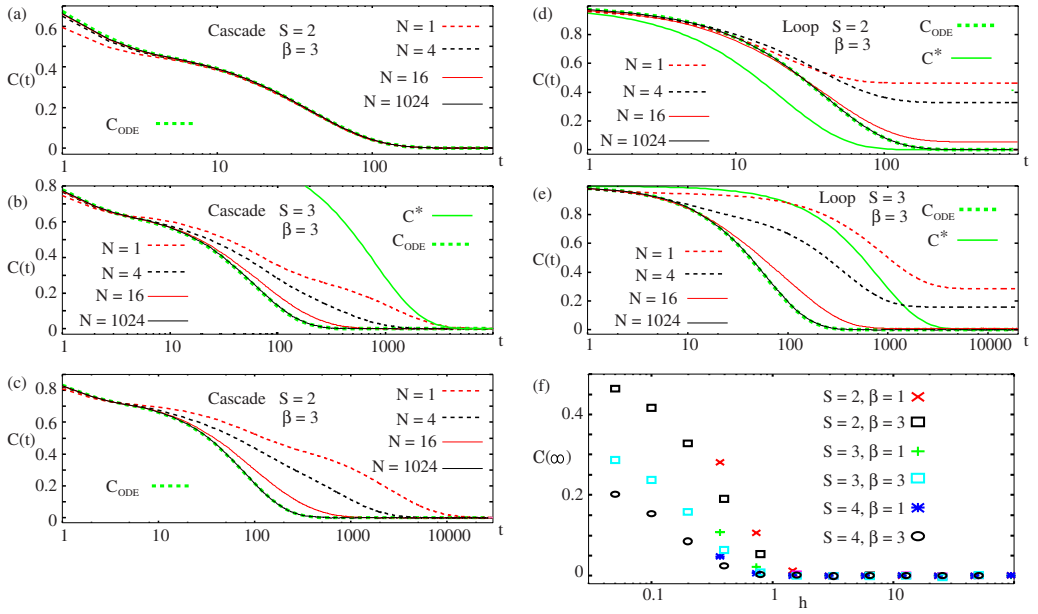

FIG. 2. (Color online) $C(t)$ of cascade systems with (a) $S=2$, (b) $S=3$, and (c) $S=4$, and loop systems with (d) $S=2$ and (e) $S=3$ for several N with $\beta=3$. (f) $C(\infty)$ as a function of h in loop systems for several β and S. C_{ODE} indicates the autocorrelations given by Eq. (4) in (a)–(c) and Eq. (3) in (d) and (e). $C^*=\exp(-e^{-\beta V}t)$ in (d), and $C^*=\exp[-(e^{-2\beta V}/2)t]$ in (b) and (e) with $\beta=3$ ($V=1$).

This is because the state $(p_1,p_2,\ldots,p_S)=(0,0,\ldots,0)$ cannot be reached from other states, whereas the state cannot move to any other states. Hence, the steady distribution from the initial conditions without $(p_1,p_2,\ldots,p_S)=(0,0,\ldots,0)$ deviates from the continuum limit. This deviation becomes prominent as N becomes smaller. For example, for $N=1$ and $V_i=V$, the distribution from the initial condition without $(p_1,p_2,\ldots,p_S)=(0,0,\ldots,0)$ is given by $\langle p_i\rangle=e^{-\beta V}(1+e^{-\beta V})^{S-1}/[(1+e^{-\beta V})^S-1]$. Note that $\langle p_i\rangle$ tends to $1/S$ with an increase in β.

III. SIMULATION RESULTS

In this section, we present the results of stochastic simulations and show the dependence of the relaxation process on the number of molecules N and the inverse temperature β. For simplicity, we consider V_i to be uniform for all species $(=V)$; however, this assumption can be relaxed.

Numerical simulations are carried out by iterating the following stochastic processes. (i) We randomly pick up a pair of molecules, say, molecules 1 and 2. (ii) Molecule 1 is transformed with its reaction rate (if it is P, it is transformed to R, and vice versa) if molecule 2 can catalyze the reaction of molecule 1. In the cascade case, there is a reaction that progresses without a catalyst and, in this case, if molecule 1 is the one that reacts without a catalyst, then it is transformed with the reaction rate independently of molecule 2. Here, a unit time is defined as the time span in which the above processes for catalytic reactions are repeated SN times. In each unit time, each molecule is picked up on average to check if the transformation occurs. In the following, we focus on the behavior of the system after a sufficiently long time from the initial time where the numbers of each molecule p_i and r_i are set randomly from $[0,N]$ under the constraint $p_i+r_i=N$ and $(p_1,p_2,\ldots,p_S)\neq(0,0,\ldots,0)$.

Now, we define the autocorrelation function $c(t)$ as $c(t)=\langle\Sigma_i\{[p_i(t)-p_i^{eq}][p_i(0)-p_i^{eq}]+[r_i(t)-r_i^{eq}][r_i(0)-r_i^{eq}]\}\rangle$, by scaling so that $c(t)=0$ when the equilibrium is reached. By further normalizing the function, so that it takes unity in the initial distribution, we define $C(t)\equiv c(t)/c(0)$. Figures 2(a)–2(e) show $C(t)$ of the cascade system [Figs. 2(a)–2(c)] and the loop system [Figs. 2(d) and 2(e)] for some S and N with $\beta=3$. As already discussed, $C(\infty)\to 0$ in the cascade system, whereas $C(\infty)\to 0$ for large N but $C(\infty)>0$ for small N in the loop system. Here, the value $C(\infty)$ in the loop system starts to deviate when $h=Ne^{-\beta V}$ becomes less than 1. Hence, we have plotted $C(\infty)$ of the loop system as a function of h in Fig. 2(f) for $\beta=1$ and 3. As shown, $C(\infty)>0$ holds for $h<1$ independently of β. On the other hand, in both systems, the relaxation to the equilibrium value $C(\infty)$ is drastically slowed down for small N, as compared to that for large N when $S>2$, whereas the relaxation for small N is faster when $S=2$.

To observe the dependence of the relaxation time on N, we measured the integrated relaxation time defined as $\tau=\int_0^\infty\{[C(t)-C(\infty)]/[1-C(\infty)]\}dt$. Figures 3(a) and 3(b) show τ as a function of N for $\beta=3$ with $S=2,3,4$ for the cascade [Fig. 3(a)] and loop [Fig. 3(b)] systems. For $S\geq 3$, the relaxation time τ increases by several orders of magnitude with a decrease in N in both systems. On the other hand, τ for $S=2$ does not exhibit any drastic change with the decrease in N in both systems.

This prolongation of τ for $S>2$ becomes more prominent as β is increased. From several data, τ is suggested to increase as a function of $\exp(\beta V)$. Combining N and β dependencies, we introduce a parameter $h=N\exp(-\beta V)$. The discreteness effect is dominant when $h=N\exp(-\beta V)$ is less than unity. Figures 3(c) and 3(d) show $\rho=\tau/\tau_{N\to\infty}$ as a function of h for the cascade [Fig. 3(c)] and loop [Fig. 3(d)]

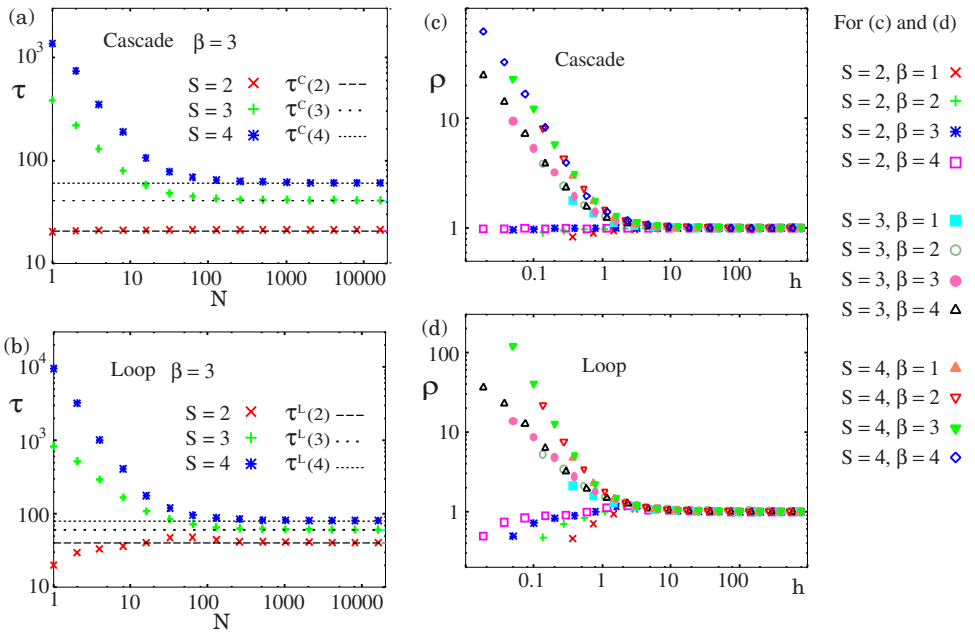

FIG. 3. (Color online) τ as a function of N in (a) cascade and (b) loop systems, and $\tau^C(S)$ and $\tau^L(S)$ for $\beta=3$ and $S=2,3,4$. ρ as a function of h in (c) cascade (d) loop systems with $S=2,3,4$ for several β.

systems for several values of β and $S=2,3,4$. For $S>2$, the deviation of ρ from the continuum limit ($\rho=1$) becomes prominent when h is below unity in both systems. The increase in ρ appears to become steeper with an increase in S. On the other hand, ρ for $S=2$ does not exhibit a drastic increase with a decrease in h.

IV. ORIGIN OF SLOW RELAXATIONS AND CROSSOVER

A. Relaxation processes for $N\to\infty$ and $N=1$

Now, we analytically estimate the enhancement in relaxation time and explain its representation in the form $h=N\exp(-\beta V)$. For this purpose, we compare the estimate by master equation analysis for small N and compare it with that from the continuum limit $N\to\infty$.

In the continuum limit, the reaction dynamics are represented by the following rate equation:

$$\dot{x}_i = x_c\left[e^{-\beta V}\left(\frac{1}{S}-x_i\right)-x_i\right], \tag{1}$$

with $x_i=p_i/SN$. Here, $x_c=1$ for $i=S$ in the cascade system, $x_c=x_1$ for $i=S$ in the loop system, and $x_c=x_{i+1}$ for $i<S$ in both systems. $x_i\to x_i^{eq}=e^{-\beta V}/[S(1+e^{-\beta V})]$ holds for $t\to\infty$. When the deviation from equilibrium $\delta x_i=x_i-x_i^{eq}$ is small, its evolution for the loop systems obeys the following linearized equation:

$$\delta\dot{x}_i = -\frac{e^{-\beta V}}{S}\delta x_i. \tag{2}$$

For the cascade system, this equation is also valid for the elements $i\neq S$, whereas $\delta\dot{x}_S=-\delta x_S$. Then, the autocorrelation function of a small fluctuation of p_i around p_i^{eq} is obtained as

$$C(t) = \exp\left(-\frac{e^{-\beta V}}{S}t\right) \tag{3}$$

for the loop system, and

$$C(t) = \frac{1}{S}\exp(-t)+\frac{S-1}{S}\exp\left(-\frac{e^{-\beta V}}{S}t\right) \tag{4}$$

for the cascade system. Indeed, these agree quite well with the simulation results for a sufficiently large N (e.g., $N=1024$ in Fig. 2.). Thus, the characteristic time of the relaxation is estimated as $\tau^L(S)\sim Se^{\beta V}$ for the loop system and $\tau^C(S)\sim\frac{1}{S}+(S-1)e^{\beta V}$ for the cascade system, which are consistent with the simulation results shown in Fig. 3.

As the other extreme limit, consider the case with $N=1$. In this case, the relaxation dynamics are dominated by a completely different process induced by the absence of catalysts whose number can often go to zero. In such cases, states are trapped at some local energy minimum that appears due to the deficiency of catalysts. Then, the hopping processes among them play an important role in the relaxation dynamics, as shown below. In the following, we focus on the cases with $S=2$ and 3 to clarify that such an effect is induced by discreteness in the molecule number. Note that, as shown in the last section, the behavior for $S\geq 3$ is distinct from that for $S=2$; in the former case, the relaxation time is enhanced by the decrease in N, in contrast to the latter case.

First, we study the loop system. When $S=2$, the system realizes three states from the initial conditions—$(p_1,p_2)=(1,0)$, $(0,1)$, and $(1,1)$—as shown in Fig. 4(a). In this case, the transition rate from the state $(1,0)$ to $(1,1)$ is estimated as follows: for this transition, a pair of molecules from the product of the first species and the resource of the second species has to be chosen. This probability is given by $\frac{1}{2}\frac{1}{2-1}$, while the reaction rate is given by $e^{-\beta V}$. In unit time, this

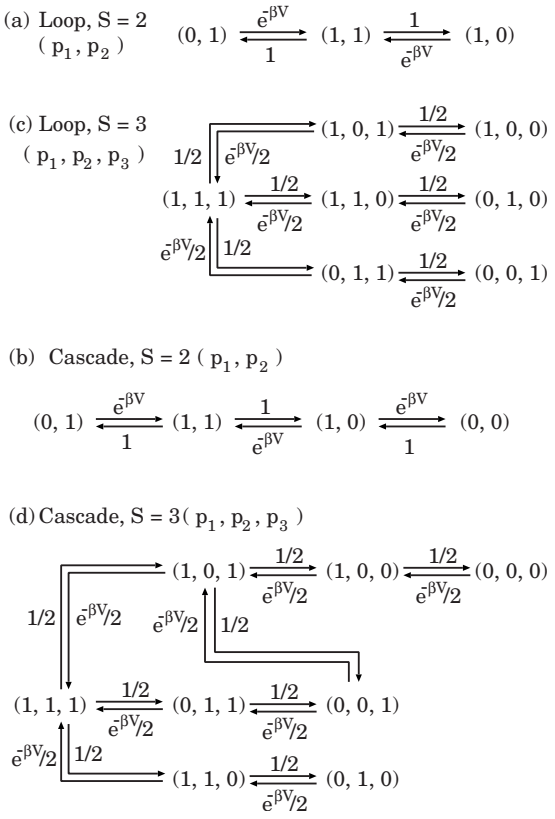

FIG. 4. (a) Illustration of transition diagrams of (a) loop system with $S=2$, (b) loop system with $S=s$, (c) cascade system with $S=2$, and (d) cascade system with $S=3$, where arrows indicate possible transitions and the values next to them specify the transition ratios.

process is iterated two times. Hence, the rate is given by $2\times\frac{1}{2}\frac{1}{2-1}e^{-\beta V}=e^{-\beta V}$. Then, the characteristic time of the correlation of each p_i is given by $\sim e^{\beta V}$, which is consistent with the results shown in Fig. 2(d).

On the other hand, for $S=3$, the system realizes seven states—$(p_1,p_2,p_3)=(1,0,0)$, $(0,1,0)$, $(0,0,1)$, $(1,1,0)$, $(1,0,1)$, $(0,1,1)$, and $(1,1,1)$—as shown in Fig. 4(b). The characteristic time of the correlation of each p_i is given by the transition time among the three branches including lowest-energy states, $(1,0,1)$-$(1,0,0)$, $(1,1,0)$-$(0,1,0)$, and $(0,1,1)$-$(0,0,1)$. Here, in order to hop from one branch to another, the system must go through the highest-energy state $(1,1,1)$ due to the restriction by the catalytic relation. Thus, the escape rate from each branch is estimated by $\sim\frac{1}{2}e^{-2\beta V}$, and the characteristic time of the correlation of each p_i is estimated as $\sim 2e^{2\beta V}$ (see Appendix A). Because the relaxation time in the continuum limit is proportional to $\exp(\beta V)$, the deviation ρ from it increases with $\exp(\beta V)$, which is consistent with the results shown in Fig. 2(e). Thus, the enhancement of the relaxation time from the continuous case is explained.

Essentially the same argument is also valid for the cascade systems. When $S=2$, the system can realize transitions among four states—$(0,1)$-$(1,1)$-$(1,0)$-$(0,0)$—as shown in Fig. 4(c). Here, $(0,1)$ is a metastable state and $(0,0)$ is the lowest-energy state. The relaxation is characterized by the escape rate from a metastable state, which is given by $\sim e^{-\beta V}$. Thus, the characteristic time of the correlation of each p_i is given by $\sim e^{\beta V}$.

On the other hand, for $S=3$, the system realizes eight states—$(p_1,p_2,p_3)=(0,0,0)$, $(1,0,0)$, $(0,1,0)$, $(0,0,1)$, $(1,1,0)$, $(1,0,1)$, $(0,1,1)$, and $(1,1,1)$—as shown in Fig. 4(d). The slowest characteristic time of the relaxation is given by the transition time from the branch $(1,1,0)$-$(0,1,0)$ since the system must go through the highest-energy state $(1,1,1)$, which is a limiting process for this case. Then, in a manner similar to the loop system with $S=3$, the characteristic time is obtained as $\sim 2e^{2\beta V}$. This gives the characteristic time of the slowest motions of the system. This estimation fits well with the numerical result shown in Fig. 2(b).

B. N and β dependencies of $C(\infty)$ and relaxation time

Next, we extend the argument of the last section to analyze the N and β dependencies of $C(\infty)$ and the relaxation time in greater detail. In particular, we explain why $h=N\exp(\beta V)\sim 1$ gives a critical value and how the amplification of relaxation time depends on h for $h<1$. Because of the simplicity due to the symmetry in the catalytic relationship, we only study loop systems; however, the argument presented below can be extended to cascade systems.

Figure 5(a) shows the transition diagram of the loop system with $S=2$, where each circle indicates each state (p_1,p_2) and the arrows indicate possible transitions. Generally, for any values of S, the transition rate from a state $(p_1,p_2,\ldots,p_i=n,p_{i+1},\ldots,p_S)$ to a state $(p_1,p_2,\ldots,p_i=n+1,p_{i+1},\ldots,p_S)$ per unit time is estimated as follows. For this transition, a pair of molecules from the resource of the ith species (R_i) and the product of the $(i+1)$th species (P_{i+1}) has to be chosen. This probability is given by $[(N-p_i)/SN][p_{i+1}/(SN-1)]$, and the reaction rate is given by $e^{-\beta V}$. Hence, the transition rate per unit time is given by

$$W^i_{n\to n+1}=\frac{(N-n)p_{i+1}}{SN-1}e^{-\beta V}.$$

Similarly, the transition rate in the opposite direction is given as

$$W^i_{n+1\to n}=\frac{(n+1)p_{i+1}}{SN-1}.$$

If the molecule number is so large or β is so small that $h=Ne^{-\beta V}\gg 1$, $W^i_{n\to n+1}>W^i_{n+1\to n}$ holds for small n and $W^i_{n\to n+1}<W^i_{n+1\to n}$ holds for large n. Then, the dominant states of the system are located in an intermediate region in the phase space $[0,N]$. For example, the intermediate gray (blue online) region in Fig. 5(a) indicates such dominant states for $S=2$. Under such conditions, $x_i=\langle p_i\rangle/SN$ obeys Eq. (1) for a sufficiently large value of N (see Appendix B).

On the other hand, if N is so small or β is so large that $h\ll 1$, $W^i_{n\to n+1}\ll W^i_{n+1\to n}$ holds for all i and n. Thus, p_i for all i tends to decrease to zero. Then, there exist S^N metastable states—$(n,0,0,\ldots,0)$, $(0,n,0,\ldots,0)$, …, $(0,0,\ldots,0,n,0,\ldots,0)$, …, and $(0,0,0,\ldots,n)$ $(1\le n\le N)$. Among them, the following S states, $(1,0,0,\ldots,0)$, $(0,1,0,\ldots,0)$, …, and $(0,0,0,\ldots,1)$, have the lowest en-

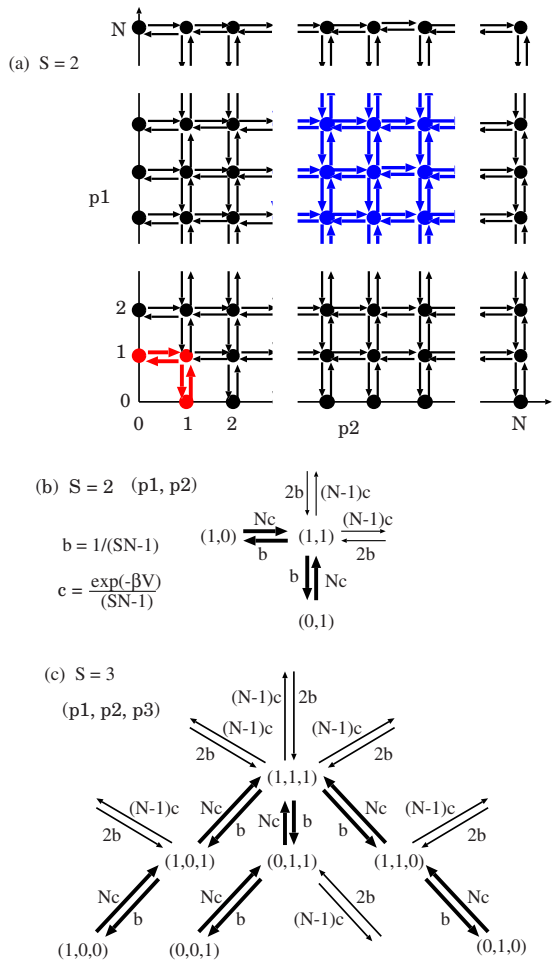

FIG. 5. (Color online) (a) Illustration of the transition diagrams for $S=2$, and effective transition diagrams for (b) $S=2$ and (c) $S=3$, where bold arrows indicate the focused transitions in the text.

ergy. For example, in the cases with $S=2$, the states $(0,p)$ and $(q,0)$ $(p,q\neq 0)$ are metastable states and (1,0) and (0,1) are the lowest-energy states.

It should be noted that the lowest-energy states are the dominant states for $h\ll 1$. The probability to realize these lowest-energy states tends to $1/S$ with an increase in β. Thus, with the increase in β, $\langle p_i\rangle$ approaches $1/S$ for small N, which indicates $C(\infty)=\text{const}>0$ for small N and large β.

Moreover, for $h\ll 1$, the transitions among lowest-energy states contribute dominantly to the relaxation process. Then, we estimate the characteristic time of the fluctuations of the system for $h\ll 1$ by considering the transition processes from one lowest-energy states such as $(0,0,\ldots,0,p_j=1,0,\ldots,0)$ to the other lowest-energy states such as $(0,0,\ldots,0,p_j=0,0,\ p_{j'}=1,0,\ldots,0)$. In the following, we consider only the cases with $S=2$ and 3. We only focus on the dynamics of p_j under the constraint that p_j has only 0 or 1, because $h\ll 1$.

First, consider the case with $S=2$. Figure 5(b) shows a detailed transition diagram around the region where p_i $(i=1,2)$ is only 0 or 1. The escape rate from (1,0) and (0,1) is given by $\sim\frac{N}{2N-1}e^{-\beta V}$. Thus, the characteristic time of the correlation of each p_i is given by

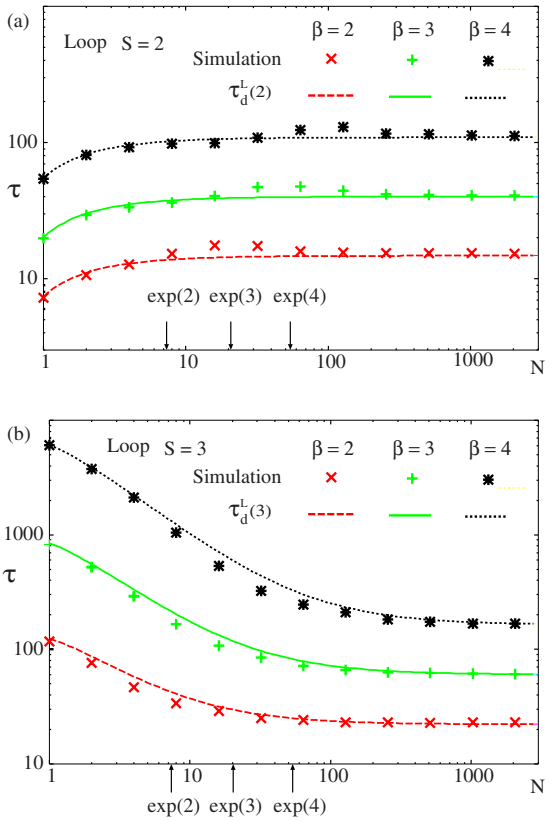

FIG. 6. (Color online) Relaxation time τ obtained from simulations (points) and its approximate analytical expression $\tau_d^L(S)$ (curves) estimated in the text. Plotted as a function of N for the loop systems with (a) $S=2$ and (b) $S=3$ with $\beta=2,3,4$. The analytical expression agrees with the simulation data both for small N, and for large N, where τ approaches a constant value expected from the rate equation. The crossover occurs at around $h=Ne^{-\beta V}\sim 1$ [$N\sim\exp(2)$, $\exp(3)$, and $\exp(4)$ for $\beta=2$, 3, and 4].

$$\tau_d^L(2)\sim\frac{2N-1}{N}e^{\beta V}, \tag{5}$$

which is consistent with the results shown in Fig. 6(a).

Next, we study the case with $S=3$. The transition diagram of the states (p_1,p_2,p_3) is shown in Fig. 5(c) when p_i $(i=1,2,3)$ takes only 0 or 1. Similar to the $N=1$ case, the characteristic time of the transition among the three branches including lowest-energy states, (1,0,1)-(1,0,0), (1,1,0)-(0,1,0), and (0,1,1)-(0,0,1) through the state (1,1,1), is considered. In a manner similar to the $N=1$ case, the transition rate from each branch is estimated by $\sim[Ne^{-\beta V}/(3N-1)][Ne^{-\beta V}/(1+Ne^{-\beta V})]=N^2e^{-\beta 2V}/[(3N-1)(1+Ne^{-\beta V})]$. Thus, the relaxation time of the fluctuation of p_1 is estimated as the decrease with N as

$$\tau_d^L(3)\sim\frac{(3N-1)(1+Ne^{-\beta V})}{N^2}e^{2\beta V}. \tag{6}$$

Considering the $e^{\beta V}$ dependence of $\tau_{N\to\infty}$, the above estimate is consistent with Fig. 6(b).

For S larger than 3, the transition diagram becomes rather complicated. However, a similar analysis should be possible to estimate the prolongation in the relaxation time.

V. SUMMARY AND DISCUSSIONS

In the present paper, the slowing down of the relaxation in reversible catalytic reaction networks induced by the smallness of molecule number is investigated as a general property of catalytic reaction networks. This prolongation of relaxation is a result of bottlenecks in reactions; these appear due to the deficiency of the catalyst required for a reaction. The number of molecules can be so small that the number of catalysts becomes zero. In this case, a pair of a substrate and the corresponding catalyst molecule species can hardly exist simultaneously. Such a constraint makes it difficult to realize a specific configuration necessary for the relaxation. The probability for realization is given by $\exp(-\beta E_b)$, with E_b as the corresponding effective energy barrier to realize such rare conditions, or the sum of such energy barriers. This bottleneck energy is generally different from the energy gap in the continuum limit that is obtained from the relaxation time of the rate equation (ordinary differential equation). Thus, the relaxation time at a small molecule number deviates from the continuum case by the factor $\exp(\beta\delta E)$ with an appropriate effective energy difference δE.

By considering the models of simple catalytic reaction networks consisting of resource chemicals of S species and the corresponding products, we have demonstrated this deviation of relaxation time from both direct simulations and analysis by using master equation. From the numerical and analytical estimates, $V \leq E_b \leq 2V$ and $0 \leq \delta E \leq V$ for $S=3$, where V is the energy gap between the resource and the product chemicals. For $S>2$, in general, the prolongation of the relaxation time becomes prominent when $h=N\exp(-\beta V)$ is less than unity, and its amplification ratio from the continuum limit is represented as a function of S and h. Note that the cascade system in the $N=1$ case is equivalent to the "asymmetrically constrained Ising chain" (ACIC), hierarchically constrained Ising model, or east model, which are studied as simple abstract models for glassy states [23–25]. Following the interpretation therein, the increase in relaxation time at $h<1$ as a result of the decrease in N or temperature may be regarded as a type of glass transition. According to the recent studies on ACIC, the correlation time of the motion of p_1 (not the relaxation time of the total system) is estimated as $\tau_1 \sim (1+2e^{\beta V})^k$, where the integer k obeys $2^{(k-1)} < S \leq 2^k$ [24,25]. In cases with $S=2,3,4$, this fact is consistent with our estimate of the relaxation time of the cascade system with $N=1$. The estimation of δE as a function of S and h for general cases both for cascade and loop systems is an important issue that should be studied in the future.

In addition to the slowdown in relaxation, the equilibrium distribution deviates in a network called a loop system, where all the reactions are catalyzed by one of the products. The constraint that the numbers of a certain pair of chemical species cannot simultaneously be zero leads to the deviation of the average distribution of molecule numbers from the continuum limit. Again, this deviation becomes prominent when h is less than unity.

Although we have adopted simple network motives to analyze the relaxation, the prolongation of relaxation time is quite general in catalytic reaction networks. Catalytic bottlenecks often appear as the number of molecules is decreased in a large variety of reaction networks in which catalysts are synthesized within [21,22]. The present study can provide a basis for the general case with complex networks, as the motives here are sufficiently small and can exist within such complex networks.

Biochemical reactions generally progress in the presence of catalysts that are themselves synthesized as products of such reactions. These reactions form a network of a variety of chemical species. Here, the molecule number of each species is generally not very large. Hence, the slow relaxation process and deviation from equilibrium discussed in this study may underlie intracellular reaction processes. Moreover, the present network motives are so simple that they are suggested to exist in biochemical networks. We also note that the resource and product in our model can be interpreted as nonexcited and excited states of enzymatic molecules. Indeed, many molecules are known to exhibit catalytic activity only when they are in an excited state, which can help other chemicals to switch to an excited state. In fact, such networks with mutual excitation are known in signal-transduction networks [26–28], where the present slow relaxation mechanism may be relevant to sustain the excitability of a specific enzyme type over a long time span. It is important to pursue the relevance of the present mechanism in cell-biological problems by considering more realistic models in the future.

We also note that not only the discreteness in the molecule number but also the negative correlation between a substrate and the corresponding catalyst within a reaction network or in a spatial concentration pattern suppresses the relaxation process [2,3,21,22]. The present mechanism due to discreteness may work synergetically with the earlier mechanism to further suppress the relaxation to equilibrium. The construction of reaction networks to achieve slower relaxation together with the network analysis will be an important issue in the future.

ACKNOWLEDGMENTS

The authors would like to thank Shinji Sano for informing us of his finding on the prolongation of relaxation in reaction networks due to the discreteness in molecule numbers, which triggers the present study. A.A. was supported in part by a Grant-in-Aid for Young Scientists (B) (Grant No. 19740260) from MEXT of Japan.

APPENDIX A

We define the probability that the states in the branch (1,0,1)-(1,0,0) are realized as $Q_{1,0,0}$. Then, the probability to realize the state (1,0,1) is given by $[e^{-\beta V}/(1+e^{-\beta V})]Q_{1,0,0}$. Here, the transition rate from (1,0,1) to (1,1,1) is given by $e^{-\beta V}/2$. Then, the probability current from the branch

(1,0,1)-(1,0,0) is estimated by $\sim(e^{-\beta V}/2)[e^{-\beta V}/(1+e^{-\beta V})]Q_{1,0,0}\sim 1/2e^{-2\beta V}Q_{1,0,0}$ ($e^{-\beta V}\ll 1$). Because of the symmetry among the catalytic reactions, the probability currents from the other branches are obtained in the same way to get the same form. Thus, the escape rate from each branch is estimated by $\sim\frac{1}{2}e^{-2\beta V}$.

APPENDIX B

We define the probability that $p_i=n$ as Q_n^i, and the joint probability to realize $p_i=n$ and $p_{i+1}=m$ as $Q_{n,m}^i$. Here, $Q_n^i=\Sigma_{m=0}^N Q_{n,m}^i$ and $Q_{n,m}^i=Q_n^i Q_m^{i+1}$. Then the time evolution of $Q_{n,m}^i$ follows

$$\dot{Q}_{n,m}^i=\frac{m}{SN-1}\{[N-(n-1)]e^{-\beta V}Q_{n-1,m}^i+(n+1)Q_{n+1,m}^i - nQ_{n,m}^i-(N-n)e^{-\beta V}Q_{n,m}^i\}. \tag{B1}$$

Then, we obtain

$$\dot{Q}_n^i=\frac{\langle p_{i+1}\rangle}{SN-1}\{[N-(n-1)]e^{-\beta V}Q_{n-1}^i + (n+1)Q_{n+1}^i-nQ_n^i-(N-n)e^{-\beta V}Q_n^i\}, \tag{B2}$$

where $\langle p_i\rangle=\Sigma_{n=0}^N nQ_n^i$ ($\langle p_{i+1}\rangle=\Sigma_{m=0}^N mQ_m^{i+1}$). Using this equation, we obtain the time evolution of $\langle p_i\rangle$ as

$$\langle\dot{p}_i\rangle=\frac{\langle p_{i+1}\rangle}{SN-1}[-\langle p_i\rangle+(N-\langle p_i\rangle)e^{-\beta V}]. \tag{B3}$$

This implies that $x_i=\langle p_i\rangle/SN$ obeys Eq. (1) for a sufficiently large value of N.

[1] K. Kang and S. Redner, Phys. Rev. Lett. **52**, 955 (1984); M. Yang, S. Lee, and K. J. Shin, *ibid.* **79**, 3783 (1997); I. V. Gopich, A. A. Ovchinnikov, and A. Szabo, *ibid.* **86**, 922 (2001); D. Pines and E. Pines, J. Chem. Phys. **115**, 951 (2001).

[2] A. Awazu and K. Kaneko, Phys. Rev. Lett. **92**, 258302 (2004).

[3] A. Awazu and K. Kaneko, Phys. Rev. E **80**, 041931 (2009).

[4] N. Olsson, E. Piek, P. ten Dijke, and G. Nilsson, J. Leukoc Biol. **67**, 350 (2000).

[5] P. Guptasarma, BioEssays **17**, 987 (1995).

[6] H. H. McAdams and A. Arkin, Trends Genet. **15**, 65 (1999).

[7] Y. Togashi and K. Kaneko, Phys. Rev. Lett. **86**, 2459 (2001); J. Phys. Soc. Jpn. **72**, 62 (2003); J. Phys.: Condens. Matter **19**, 065150 (2007).

[8] J. Ohkubo, N. Shnerb, and D. A. Kessler, J. Phys. Soc. Jpn. **77**, 044002 (2008).

[9] A. Awazu and K. Kaneko, Phys. Rev. E **76**, 041915 (2007).

[10] A. Awazu and K. Kaneko, Phys. Rev. E **80**, 010902(R) (2009).

[11] B. Hess and A. S. Mikhailov, Science **264**, 223 (1994); J. Theor. Biol. **176**, 181 (1995).

[12] P. Stange, A. S. Mikhailov, and B. Hess, J. Phys. Chem. B **104**, 1844 (2000).

[13] N. M. Shnerb, Y. Louzoun, E. Bettelheim, and S. Solomon, Proc. Natl. Acad. Sci. U.S.A. **97**, 10322 (2000).

[14] Y. Togashi and K. Kaneko, Physica D **205**, 87 (2005).

[15] G. Marion, X. Mao, E. Renshaw, and J. Liu, Phys. Rev. E **66**, 051915 (2002).

[16] V. P. Zhdanov, Eur. Phys. J. B **29**, 485 (2002).

[17] T. Dauxois, F. Di Patti, D. Fanelli, and A. J. McKane, Phys. Rev. E **79**, 036112 (2009).

[18] K. Kaneko, Adv. Chem. Phys. **130**, 543 (2005).

[19] C. Furusawa and K. Kaneko, Phys. Rev. Lett. **90**, 088102 (2003).

[20] C. Furusawa *et al.*, Biophysics **1**, 25 (2005).

[21] S. Sano, Master thesis, University of Tokyo, 2009 (in Japanese).

[22] S. Sano, A. Awazu, and K. Kaneko (unpublished).

[23] J. Jäckle and S. Eisinger, Z. Phys. B: Condens. Matter **84**, 115 (1991).

[24] F. Mauch and J. Jäckle, Physica A **262**, 98 (1999).

[25] P. Sollich and M. R. Evans, Phys. Rev. Lett. **83**, 3238 (1999); Phys. Rev. E **68**, 031504 (2003).

[26] A. Goldbeter and D. K. Koshland, Jr., Proc. Natl. Acad. Sci. U.S.A. **78**, 6840 (1981); J. Biol. Chem. **259**, 4441 (1984).

[27] A. Levchenko and P. A. Iglesias, Biophys. J. **82**, 50 (2002).

[28] W. Ma, A. Trusina, H. El-Samad, W. A. Lim, and C. Tang, Cell **138**, 760 (2009).